ELSEVIER

Journal of Biomechanics 40 (2007) 2222–2229

JOURNAL OF BIOMECHANICS

www.elsevier.com/locate/jbiomech
www.JBiomech.com

Evaluation of the carpal tunnel based on 3-D reconstruction from MRI

Jeremy P.M. Mogk[a], Peter J. Keir[b,*]

[a]School of Kinesiology & Health Science, York University, Toronto, Ont., Canada
[b]Department of Kinesiology, McMaster University, 1280 Main Street West, Hamilton, Ont., Canada L8S 4K1

Accepted 19 October 2006

Abstract

While deviated wrist postures have been linked to the development of carpal tunnel syndrome, the relative contributions of posture-related changes in size, shape and volume of the carpal tunnel contribute to median nerve compression are unclear. The purpose of this study was two-fold: (1) to reconstruct the carpal tunnel from MRI data in neutral and non-neutral (30° extension, 30° flexion) wrist postures, and (2) to evaluate errors associated with off-axis imaging. Three-dimensional reconstruction of the carpal tunnels of 8 volunteers from the university community revealed that the orientation of the carpal tunnel was not directly explained by external wrist angle. The average orientation of the carpal tunnel was extended in all postures, ranging from $25^\circ \pm 9^\circ$ in extension, $13^\circ \pm 5^\circ$ in neutral and $4^\circ \pm 4^\circ$ in the flexed wrist. Changing the orientation of the imaging plane to be perpendicular to the reconstructed carpal tunnel revealed that axial images overestimated cross-sectional area by an average of nearly 10% in extension, 4% in neutral and less than 1% in flexion. Similarly, adjusting the imaging plane to be perpendicular to external wrist angle overestimated cross-sectional area by an average of 2% in extension, 4% in neutral and 24% in flexion. Distortion of the carpal tunnel shape also became evident with rotation of the imaging plane. The data suggest that correction for the orientation of the carpal tunnel itself to be more appropriate than relying on external wrist angle. Computerized reconstruction provided detailed anatomic visualization of the carpal tunnel, and has created the framework to develop a biomechanical model of the carpal tunnel. Similar reconstruction of the tissue structures passing through (median nerve and flexor tendons) and entering the carpal tunnel (muscle tissue) will enable evaluation and partitioning of median nerve injury mechanisms.

Keywords: Carpal tunnel syndrome; MRI; Cross-sectional area; Volume; Wrist; Three-dimensional reconstruction; Modeling

1. Introduction

Although carpal tunnel syndrome (CTS) is the most common peripheral entrapment neuropathy, the etiology of work-related CTS remains elusive (Rempel and Diao, 2004). Compression of the median nerve can result from mechanical impingement or increased hydrostatic pressure, both of which have been shown to occur with deviation from a neutral wrist posture (Smith et al., 1977; Gelberman et al., 1981; Rojviroj et al., 1990; Weiss et al., 1995; Keir et al., 1997; Werner et al., 1997; Luchetti et al., 1998). It has also been demonstrated that the cross-sectional area (CSA) of the carpal tunnel changes with deviation from a neutral wrist posture (Skie et al., 1990; Yoshioka et al., 1993; Allmann et al., 1997; Bower et al., 2006). Changes in carpal tunnel pressure are a function of tunnel volume as well as the volume of its contents. While changes in pressure and shape have provided insight into median nerve trauma, integration of these concepts is necessary to test hypotheses of median nerve compression.

Magnetic resonance imaging (MRI) provides a non-invasive method by which osseous and soft tissue structures can be examined. By tracing the structures of the carpal tunnel from images, CSA may be determined throughout the tunnel (Cobb et al., 1992; Pierre-Jerome et al., 1997; Bower et al., 2006). Mathematical integration of these CSAs can then be used to calculate the volume of the carpal tunnel (Richman et al., 1987, 1989; Pierre-Jerome et al., 1997; Bower et al., 2006) as well as its contents (Cobb et al., 1992; Bower et al., 2006). However, only recently

*Corresponding author. Tel.: +905 525 9140x23543; fax: +905 523 6011.
E-mail address: pjkeir@mcmaster.ca (P.J. Keir).

0021-9290/$ - see front matter © 2006 Elsevier Ltd. All rights reserved.
doi:10.1016/j.jbiomech.2006.10.033

have carpal tunnel volumes and contents/tunnel ratios been calculated in non-neutral wrist postures (Bower et al., 2006), prompting the current study.

Carpal tunnel imaging studies in non-neutral wrist postures have typically examined changes in dimensions at specific bony landmarks relating CSA to potential sites of impingement or changes in carpal tunnel pressure (Skie et al., 1990; Yoshioka et al., 1993; Allmann et al., 1997). However, unless scanning planes are changed with wrist posture, to remain perpendicular to the carpal tunnel, axial MRI in deviated postures likely requires correction for distortion (Bower et al., 2006). This concept is supported by an analysis of the finger flexor tendons which demonstrated that they pass through the tunnel at a smaller angle than the external wrist angle (Keir and Wells, 1999). However, imaging studies of the carpal tunnel often do not report imaging (scan) plane orientation relative to wrist posture, leaving potential distortion in question. Moreover, discussion of the potential implications of image alignment on carpal tunnel size and shape has not appeared in the literature. While examination of non-neutral postures is essential to understanding the mechanisms of CTS, the potential error inherent in imaging deviated postures must be evaluated.

Computerized "reconstruction" has been performed to assess anatomic characteristics of the carpal tunnel (Pierre-Jerome et al., 1997) and its contents in a neutral wrist posture (Buitrago-Téllez et al., 1998). A recent study in our laboratory provided a detailed analysis of posture-dependent anatomical differences in CSA and volume; suggesting the need for improved assessment of CSAs (Bower et al., 2006). The purpose of the current investigation was two-fold: (1) to create computerized visual analog reconstructions of the carpal tunnel from existing MRI data in three wrist postures, and (2) to use the reconstructions to evaluate errors associated with off-axis imaging.

2. Methods

MRI data for eight individuals (4 male, 4 female) from a previous study (Bower et al., 2006) were imported into Maya™ software (v5.0, Alias®, Toronto, Canada) to graphically reconstruct the carpal tunnel. Male participants were a mean age of 27.0 (SD 1.8) years, 174.6 (10.8) cm tall, with a mass of 73.0 (3.2) kg, and wrist circumference of 17.1 (0.3) cm. Female participants were 25.5 (2.4) years of age, 161.3 (10.9) cm tall, with a mass of 60.2 (1.9) kg, and wrist circumference of 14.7 (0.8) cm. All volunteers were from the university community, self-identified as healthy and non-symptomatic at the time of testing, and reported no history of hand, wrist or forearm dysfunction. This resulted in comparison data from two methods for carpal tunnel area and volume, labeled (i) "MRI" (from Bower et al., 2006), and (ii) "reconstruction" from the current study (Fig. 1). The MRI dataset for each individual consisted of contiguous wrist scans (3 mm slices) from the radial styloid to the metacarpal bases, in 3 splinted wrist postures (30° flexion, neutral and 30° extension). All axial images were acquired with the imaging plane oriented perpendicular to the longitudinal axis of the forearm. The dorsal and palmar tunnel borders were defined as the inner surface of the palmar and transverse carpal ligaments, respectively. Often considered "pillars" of the carpal tunnel, proximal and distal boundaries were defined as the proximal aspect of the pisiform and the distal aspect of the hook of the hamate, as in previous studies (e.g. Yoshioka et al., 1993).

2.1. Reconstruction of osseous and soft tissue structures

Outlines of the carpal tunnel for each MRI slice were imported into Maya™ and used to reconstruct the carpal tunnel surfaces using a non-uniform rational B-spline function ("NURBS," a form of Bézier spline). The tunnels of all 8 wrists were reconstructed in neutral, 30° flexion and 30° extension (24 reconstructions in total) to quantitatively assess tunnel orientation and the effects of out-of-plane imaging (distortion) on CSA measures (Section 2.2.2). The number of x–y coordinates of each outline was reduced to smooth each digitized contour prior to surface reconstruction without altering their overall shape.

2.2. Reconstruction evaluation

2.2.1. Cross-sectional area (CSA)

To mimic the original MRI acquisition parameters, a fixed "axial" measurement plane, or "cut-line", was created perpendicular to the long axis of the forearm (termed "CSA_{axial}"). Calculations progressed from the proximal border of the pisiform toward the distal border of the hook of the hamate in 3 mm increments, to simulate slice thickness (Fig. 2).

2.2.2. Out-of-plane image distortion

The effect of off-axis imaging on CSA was evaluated by altering the cut-line orientation to two other angles in addition to the axial plane, based perpendicular to: (1) the external wrist angle ("wrist"—CSA_{wrist}); and (2) the angle of the carpal tunnel ("tunnel"—CSA_{tunnel}) (Fig. 3). Wrist angle was measured between the long axes of the radius and second metacarpal (Fig. 3b). Thus, CSA_{wrist} is equivalent to CSA_{axial} in the neutral (0°) wrist posture. Carpal tunnel angle was defined as a straight line representing the dorsal surface of the carpal tunnel (Fig. 3c). To achieve the alternate slice orientations, axial slices were rotated about their midpoint. CSAs were evaluated relative to CSA_{axial} at each corresponding position along the tunnel (average relative difference for each tunnel), and carpal tunnel orientation was compared to wrist angle in each posture.

2.3. Statistical analysis

Repeated measures ANOVAs were performed using STATISTICA (v6.0, StatSoft, Inc., Tulsa, OK) to evaluate the accuracy of tunnel reconstructions (based on CSA_{axial}), and the effects of wrist posture and cut-line orientation on the relative changes in carpal tunnel CSA. Significant ANOVA results ($p = 0.01$) are presented with an F-statistic, and were further evaluated using planned contrast analyses (least-squares means). Potential gender effects were not examined due to the small number of participants.

3. Results

For clarity, reference to "MRI data" corresponds with measures determined by Bower et al. (2006) directly from axial MRI, while carpal tunnel "reconstruction" refers to the surfaces generated using Maya™ from the same MRI data of 8 wrists. Measures for each technique and other features are outlined in Fig. 1.

3.1. Carpal tunnel cross-sectional area and the effects of slice orientation

CSA_{axial} values from carpal tunnel reconstructions were an average of $0.3\% \pm 0.7\%$ smaller than CSA calculated from MRI data (all slices; Bower et al., 2006), but were not

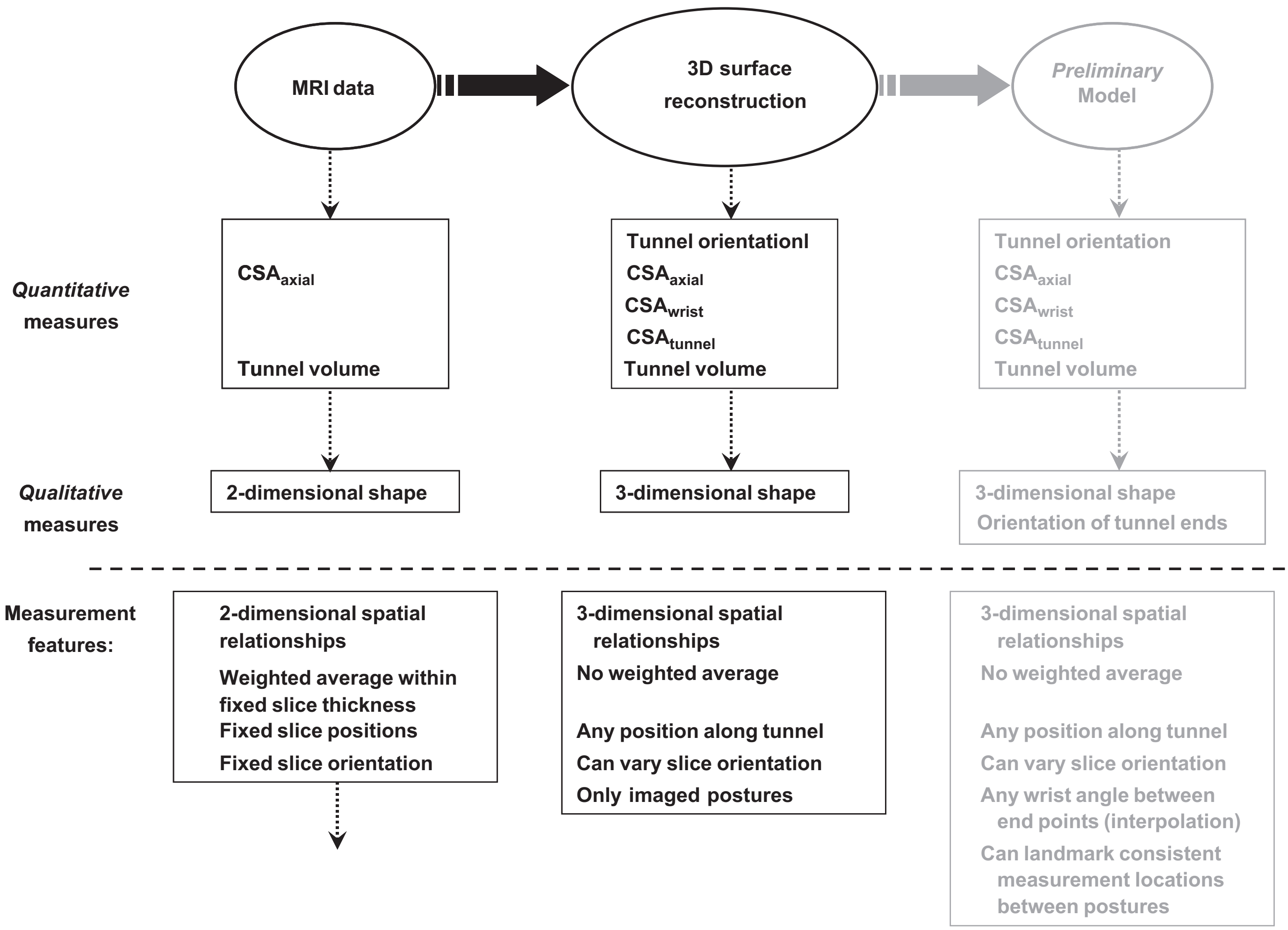

Fig. 1. The process of using MRI data to construct and validate the three-dimensional reconstructions of the carpal tunnel. Validation measures used for comparison are aligned horizontally, and separated into quantitative and qualitative. The bottom row provides a comparison of measurement features provided by each data source. The stand alone model under development (Mogk and Keir, 2006) is included in gray to illustrate the progression.

statistically different. CSA measured from each of the reconstructed tunnels ($n = 8$, for each posture) varied significantly with the interaction between wrist posture and slice orientation ($F_{4,24} = 26.6$, $p < 0.0001$). Rotation of the imaging plane perpendicular to the external wrist angle (CSA_{wrist}; Figs. 3b and 4) in the extended posture resulted in an average CSA decrease of 5.4%±7.7% (as much as 15%), relative to CSA_{axial} ($p < 0.01$). By definition, CSA_{wrist} for the neutral wrist posture is the same as CSA_{axial}. In flexion, CSA_{wrist} measured an average of 22.6%±8.3% larger than CSA_{axial} ($p < 0.001$). Orienting the "cut-line" perpendicular to the dorsal surface of the tunnel (CSA_{tunnel}, Fig. 4c) resulted in values similar to CSA_{wrist} in extension (7.3%±4.9% smaller than CSA_{axial}). CSA_{tunnel} values indicated a 3.1%±3.3% decrease from CSA_{axial} for the neutral wrist posture (as much as 11%). In flexion, CSA_{tunnel} was similar to CSA_{axial} (0.5%±1.1% smaller), but significantly smaller than CSA_{wrist} ($p = 0.001$). Slice orientation also affected the shape of each slice, as seen in Fig. 4.

3.2. Carpal tunnel orientation

The average carpal tunnel orientation was extended regardless of wrist angle, as determined by a straight line along the dorsal surface of each tunnel reconstruction (Fig. 2). The amount of extension was 25°±9° with the wrist extended, 13°±5° in neutral and 4°±4° with the wrist flexed (Table 1 and Fig. 4). Carpal tunnel orientation using this technique did not differ significantly from the mean angle using successive CSA centroids throughout the tunnel length (Table 1).

3.3. Carpal tunnel volume

Reconstructed tunnel volumes were an average of 0.4%±0.6% smaller than those determined using trapezoidal integration of digitized MRI (Bower et al., 2006), but were not statistically different. Mean tunnel volume decreased in flexed and extended postures for

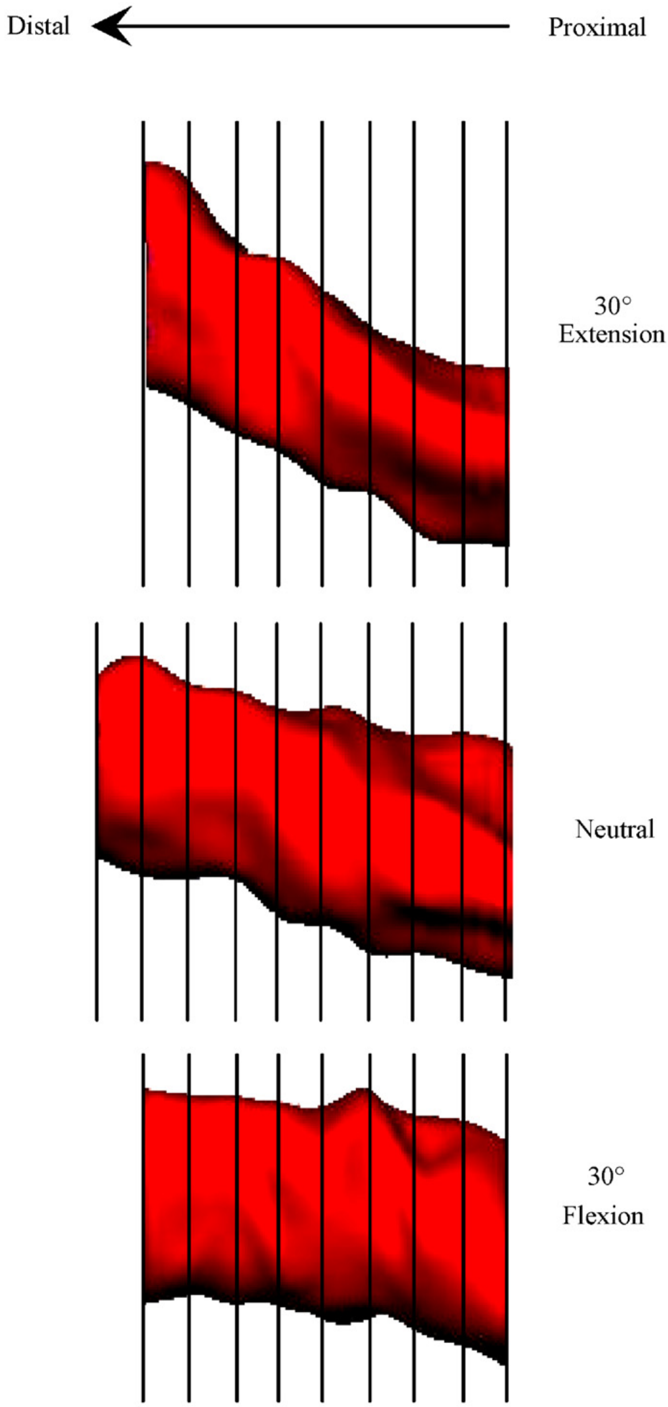

Fig. 2. Tunnel reconstructions (from one representative individual) in extended, neutral and flexed postures (top to bottom). Lines represent the "cut-lines" used to measure CSA_{axial}, mimicking axial MRI scans at 3 mm increments. Note there are more slices indicated in neutral than either extension or flexion due the requirement that transection of both the dorsal and palmar surfaces was necessary to calculate CSA_{axial}.

males, but increased for females (Table 2). This is likely due to the number of slices obtained in each posture which ranged from 5 to 9, depending on the size of the individual.

4. Discussion

This study represents an initial step in the development of a three-dimensional biomechanical model of the carpal tunnel and wrist. By improving the anatomic fidelity of the carpal tunnel beyond previous work (Pierre-Jerome et al., 1997), we were able to evaluate posture-related orientation of the carpal tunnel, as well as potential imaging errors. Three-dimensional carpal tunnel reconstruction revealed that tunnel orientation is not directly reflected by external wrist angle. In addition, to ensure physiologically accurate cross-sections, current data support aligning MRI slices perpendicular to the carpal tunnel rather than external wrist angle. The reconstruction process generated a continuous image of the tunnel and provided valuable visualization in multiple perspectives.

The benefit of the reconstruction process was immediately obvious as it permitted visualization of carpal tunnel orientation in each wrist posture, which was otherwise not possible from axial images. Carpal tunnel orientation tended toward extension in all 8 individuals, being more extended than the external wrist angle in both neutral and 30° flexed postures (13° and 4°, respectively) while slightly less than the 30° extended wrist angle (25°). While this phenomenon has not been previously reported, a past MRI study noted that the flexor tendons formed an "angle" 50–65% of external wrist angle (Keir and Wells, 1999). Discrepancies between tunnel and wrist orientation may reflect changes in palmar intercarpal ligament geometry due to individual carpal bone movement. While it has yet to be fully examined, interactions between the flexor tendons as they pass through the carpal tunnel may also affect carpal tunnel orientation (Keir and Wells, 1999). Measurement of carpal tunnel orientation was possible as the dorsal surface tended to remain relatively straight in all postures, although some curvature was apparent in extension (Fig. 3). These carpal tunnel angles were not significantly different than the mean angle calculated using successive centroids throughout the tunnel length. The relationship between tunnel orientation and wrist angle may be of anatomic importance regarding the definition of "neutral" wrist posture. In addition, our finding of a nearly neutral tunnel orientation with wrist flexion may be physiologically relevant given that carpal tunnel pressure studies have associated lowest pressure with a neutral to slightly flexed wrist posture (Weiss et al., 1995; Keir et al., 1998). Carpal tunnel orientation will likely play a role in determining the nature of median nerve compression and force transfer from the flexor tendons.

Changes in carpal tunnel orientation with wrist posture confirmed the need to evaluate off-axis imaging distortion effects on CSA. The potential for measurement error in imaging deviated postures was recently presented as a concern, but has not been otherwise addressed in the literature (Keberle et al., 2000; Bower et al., 2006). CSA_{tunnel} reflects the true, physiological CSA of the carpal tunnel, as it corrects for tunnel orientation between wrist

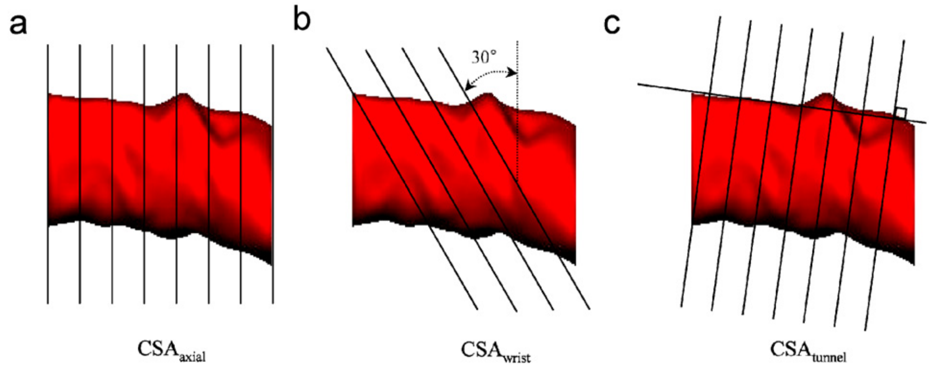

Fig. 3. Comparison of the orientation of cross-sectional area measures used to assess the effects of off-axis imaging error. Note all tunnels are one reconstructed tunnel for the same posture (30° flexion; from Fig. 2): (a) CSA_{axial} mimics standard slice orientation for axial MRI; (b) CSA_{wrist} simulates slice orientation adjusted according to wrist angle; (c) CSA_{tunnel} represents adjusted slice orientation perpendicular to the long axis of the tunnel, using the orientation of the dorsal surface. Slice increment was maintained at 3 mm for each measure.

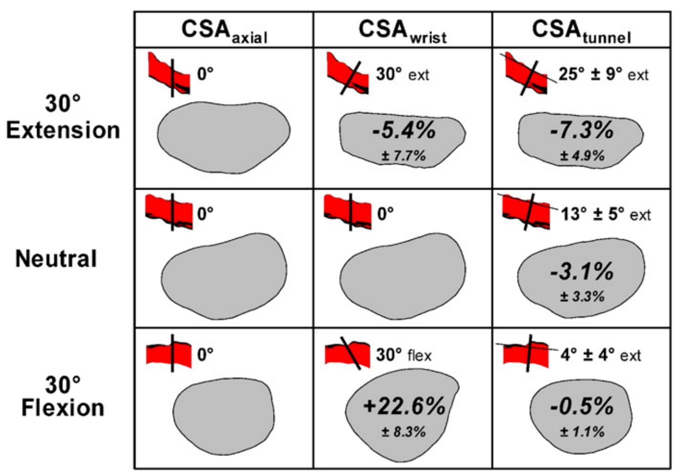

Fig. 4. Cross-sectional area as percentage difference from CSA_{axial} ($\pm$SEM) for each wrist posture ($n = 8$). Tunnel orientation is shown visually in the top left corner of each frame, with a black line representing slice orientation. Mean tunnel orientation (in degrees $\pm$ SEM) is included in the final column (CSA_{tunnel}). The gray areas show the difference in carpal tunnel shape and area at a consistent location within the carpal tunnel, from one representative individual.

postures on an individual-specific basis. Current results indicate that both CSA_{axial} and CSA_{wrist} overestimated the tunnel CSA in each of the wrist postures investigated. Consequently, restating the off-axis distortion relative to CSA_{tunnel}, rather than CSA_{axial} (as in Fig. 4), indicates an overestimation of $9.1\% \pm 6.2\%$ in extension, $3.5\% \pm 3.8\%$ in neutral and $0.6\% \pm 1.2\%$ in flexion with CSA_{axial}. CSA_{wrist} was most similar to CSA_{tunnel} in extension (1.8% larger), but was an average of 24.3% larger than CSA_{tunnel} in flexion (Table 3). Based on the current evaluation, a suggested mathematical adjustment of CSA based on external wrist angle appears to be an over-simplification (Bower et al., 2006). Interestingly, the difference between CSA_{tunnel} and CSA_{axial} was slightly larger through the distal portion of the carpal tunnel than the proximal aspect, perhaps indicating that a single angle could not account for small differences in orientation between the proximal and distal aspects of the tunnel. Remembering that CSA_{axial} in our study represents the typical orientation used in the literature, between-posture differences in CSA_{axial} (size and shape) at the proximal and distal ends of the tunnel corresponded well with those reported (Skie et al., 1990; Yoshioka et al., 1993; Allmann et al., 1997). Although imaging plane orientation is rarely defined in the literature, noted similarities with our CSA_{axial} measure indicate the likelihood that tunnel angle has not been well accounted for in previous studies. Caution should therefore be exercised when interpreting reported posture-related changes in carpal tunnel and median nerve dimensions if the imaging plane orientation is not explicitly stated (Zeiss et al., 1989; Skie et al., 1990; Yoshioka et al., 1993; Allmann et al., 1997; Monagle et al., 1999; Kuo et al., 2001). Based on the current evaluation, it is important to align the imaging plane with the carpal tunnel to reduce error. If this is not possible, CSA should be adjusted mathematically to reflect tunnel rather than wrist angle.

The reconstruction process also enabled the assessment of potential sources of variability associated with medical imaging. The smoothed reconstructed outlines (CSA_{axial}) were virtually identical (0.3% or less than 0.5 mm^2 smaller) to those determined from MRI, and could likely be considered more physiological than non-smoothed raw MRI data. The continuous nature of the reconstructions makes it possible to localize specific structures throughout the tunnel length rather than in incremental (weighted) segments from MRI (3 mm in the current study). For example, examination of one wrist revealed that CSA varied as much as 30 mm^2 at the level of the hook of the hamate depending on the exact slice location on the landmark bone. This may help explain discrepancies in carpal tunnel dimensions in the literature, and indicates the need to identify consistent landmarks, particularly when comparing between postures. Moreover, landmark selection may influence the number of slices obtained and thus the relative changes in volume between postures (Fig. 2). Further reconstruction of the carpal bones will examine

Table 1
Comparison of carpal tunnel orientation (in degrees) in each wrist posture for each wrist determined using two methods: (i) "Dorsal"—a line along the dorsal surface of each reconstructed tunnel, and (ii) "Centroid"—the average angle between successive CSA centroids throughout the length of each tunnel

	Subject	Extension (30°)		Neutral (0°)		Flexion (30°)	
		Dorsal	Centroid	Dorsal	Centroid	Dorsal	Centroid
Males	1	30	29	15	14	5	8
	2	38	32	20	19	6	7
	3	29	26	9	10	0	0
	4	20	35	12	10	7	10
	Mean (SD)	29.3 (7.4)	30.4 (4.1)	14.0 (4.7)	13.3 (4.3)	4.5 (3.1)	6.3 (4.4)
Females	5	27	23	14	6	2	−2
	6	15	18	8	15	0	0
	7	10	10	7	10	0	6
	8	30	29	20	20	12	12
	Mean (SD)	20.5 (9.5)	20.0 (8.1)	12.3 (6.0)	12.9 (5.9)	3.5 (5.7)	3.8 (6.2)
Combined	Mean (SD)	24.9 (9.2)	25.2 (8.1)	13.1 (5.1)	13.1 (4.8)	4.0 (4.3)	5.1 (5.2)

No statistical difference was noted between the two methods. Negative angles represent flexion.

Table 2
The effect of wrist posture on carpal tunnel volume and representative image slices

		Extension	Neutral	Flexion
Males	Volume	91.1% (81.9–104.9%)	100.0%	95.5% (82.4–106.2%)
	# Slices	7.75 (7–8)	8.75 (8–9)	8.75 (8–9)
Females	Volume	103.8% (89.6–125.9%)	100.0%	109.8% (99.7–119.4)
	# Slices	6.25 (5–7)	6.50 (6–8)	7.0 (6–8)
Combined	Volume	97.5% (14.6%)	100.0%	102.6% (11.6%)
	# Slices	7.0 (5–8)	7.625 (6–9)	7.875 (6–9)

Volumes are presented as a percentage of carpal tunnel volume in the neutral posture. Values in parentheses represent the range, with the exception of combined volume (SD).

Table 3
Mean difference in cross-sectional area (percent difference from CSA_{tunnel}) throughout the carpal tunnel in all three postures

	Subject	Extension		Neutral	Flexion	
		CSA_{axial}	CSA_{wrist}	CSA_{axial}	CSA_{axial}	CSA_{wrist}
Males	1	12.9	0.0	3.7	0.7	26.5
	2	18.3	−0.2	5.0	1.8	36.8
	3	6.6	0.3	0.6	0.0	17.7
	4	11.9	0.1	1.4	0.3	21.7
	Mean	12.4	0.0	2.7	0.7	25.7
	SD	4.8	0.2	2.1	0.8	8.3
Females	5	5.5	0.6	1.8	−1.1	9.2
	6	1.6	6.8	2.0	0.0	24.0
	7	1.8	6.4	1.1	0.0	18.5
	8	14.5	0.0	12.3	2.7	39.6
	Mean	5.9	3.5	4.3	0.4	22.8
	SD	6.1	3.7	5.3	1.6	12.7
Combined	Mean	9.1	1.8	3.5	0.6	24.3
	SEM	6.2	3.0	3.8	1.2	10.0

By definition, CSA_{wrist} in neutral (0°) is the same as CSA_{axial}.

changes in orientation of the proximal and distal ends of the tunnel with wrist posture.

In addition to CSA, carpal tunnel volume is an important measure due to its relationship to hydrostatic pressure. Reconstructions in the current study produced volumes virtually identical to those reported previously (Bower et al., 2006). In half of the reconstructions (4 of 8 wrists) carpal tunnel volume decreased with flexion and extension, and support reported pressure increases with deviation from neutral (Gelberman et al., 1981; Rojviroj et al., 1990; Weiss et al., 1995; Keir et al., 1997; Werner et al., 1997; Keir et al., 1998). However, tunnel reconstructions of three other wrists indicated increased volume with deviation from neutral, while the reconstructions of the final individual showed a decrease with extension and an increase in flexion. While physiological differences between individuals are inevitable, the reconstructions revealed that relative changes in volume are not simply related to the number of slices comprising each reconstruction (Table 2). For example, female data in Table 2 indicated 0.25 fewer slices in extension than neutral but a greater mean volume. This is partially attributable to the interaction between wrist size and the weighted-averaging inherent in the imaging process, and is further complicated by movement of the bony landmarks between postures. Additionally, differences in the orientation of the ends of the tunnel relative to the imaging plane can result in a less accurate estimate of volume due to missing volume beyond the end slices which intersect both palmar and dorsal tunnel surfaces (Fig. 3b, c). Without further reconstruction of the carpal bones, it is difficult to speculate how the number of slices and their orientation relative to the carpal tunnel might affect volume. Further modeling followed by detailed analysis of these specific factors is currently being completed (Mogk and Keir, 2006). Furthermore, the apparent complexity of the above relationships combined with lumbrical and finger flexor muscle incursion during wrist and finger movement (Cobb et al., 1995, 1996; Keir and Bach, 2000) strongly suggests the need to incorporate modeling of other soft tissues in the carpal tunnel to partition pressure and impingement as mechanisms of median nerve injury.

Carpal tunnel reconstruction demonstrated a method by which carpal tunnel orientation and the errors associated with standard MRI could be quantified, and laid the framework for future testing of mechanical hypotheses of median nerve injury. Reconstruction allowed improved visualization of the carpal tunnel anatomy and better quantification of dimensions than traditional two-dimensional MRI analysis. While the current investigation concentrated on carpal tunnel dimensions, the error assessment results are applicable to any imaging data. Further development of the model will incorporate carpal bones to enable more detailed modeling of the carpal tunnel and will facilitate the examination of factors that contribute to median nerve compression, including the relationship between volume and pressure, impingement and force transfer from the flexor tendons.

Acknowledgements

Special thanks to Cory Mogk for his expertise with Maya^{TM} software. This study was supported by the Natural Sciences and Engineering Research Council (NSERC grant #217382).

References

Allmann, K.H., Horch, R., Uhl, M., Gufler, H., Altehoefer, C., Stark, G.B., Langer, M., 1997. MR imaging of the carpal tunnel. European Journal of Radiology 25, 141–145.

Bower, J.A., Stanisz, G.J., Keir, P.J., 2006. An MRI evaluation of carpal tunnel dimensions in healthy wrists: implications for carpal tunnel syndrome. Clinical Biomechanics 21, 816–825.

Buitrago-Téllez, C.H., Horch, R., Allmann, K.H., Stark, G.B., Langer, M., 1998. Three-dimensional computed tomography reconstruction of the carpal tunnel and carpal bones. Plastic and Reconstructive Surgery 101 (4), 1060–1064.

Cobb, T.K., Dalley, B.K., Posteraro, R.H., Lewis, R.C., 1992. Establishment of carpal contents/canal ratio by means of magnetic resonance imaging. Journal of Hand Surgery 17A, 843–849.

Cobb, T.K., An, K.N., Cooney, W.P., 1995. Effect of lumbrical muscle incursion within the carpal tunnel on carpal tunnel pressure: a cadaveric study. Journal of Hand Surgery 20A, 186–192.

Cobb, T.K., Cooney, W.P., An, K.N., 1996. Aetiology of work-related carpal tunnel syndrome: the role of lumbrical muscles and tool size on carpal tunnel pressures. Ergonomics 39, 103–107.

Gelberman, R.H., Hergenroeder, P.T., Hargens, A.R., Lundborg, G.N., Akeson, W.H., 1981. The carpal tunnel syndrome: a study of carpal canal pressures. Journal of Bone and Joint Surgery 63A, 380–383.

Keberle, M., Jenett, M., Kenn, W., Reiners, K., Peter, M., Haerten, R., Hahn, D., 2000. Technical advances in ultrasound and MR imaging of carpal tunnel syndrome. European Radiology 10 (7), 1043–1050.

Keir, P.J., Bach, J.M., 2000. Flexor muscle incursion into the carpal tunnel: a mechanism for increased carpal tunnel pressure? Clinical Biomechanics 15, 301–305.

Keir, P.J., Wells, R.P., 1999. Changes in geometry of the finger flexor tendons in the carpal tunnel with wrist posture and tendon load: an MRI study on normal wrists. Clinical Biomechanics 14 (9), 635–645.

Keir, P.J., Wells, R.P., Ranney, D.A., Lavery, W., 1997. The effects of tendon load and posture on carpal tunnel pressure. Journal of Hand Surgery 22A, 628–634.

Keir, P.J., Bach, J.M., Rempel, D.M., 1998. Effects of finger posture on carpal tunnel pressure during wrist motion. Journal of Hand Surgery 23A, 1004–1009.

Kuo, M.H., Leong, C.P., Cheng, Y.F., Chang, H.W., 2001. Static wrist position associated with least median nerve compression: sonographic evaluation. American Journal of Physical Medicine and Rehabilitation 80 (4), 256–260.

Luchetti, R., Schoenhuber, R., Nathan, P., 1998. Correlation of segmental carpal tunnel pressures with changes in hand and wrist positions in patients with carpal tunnel syndrome and controls. Journal of Hand Surgery 23B, 598–602.

Mogk, J.P.M., Keir, P.J., 2006. Modeling posture-related changes in carpal tunnel volume. In: Proceedings of the 14th Biennial Conference for the Canadian Society for Biomechanics, Waterloo, Ontario.

Monagle, K., Dai, G., Chu, A., Burnham, R.S., Snyder, R.E., 1999. Quantitative MR imaging of carpal tunnel syndrome. American Journal of Roentgenology 172, 1581–1586.

Pierre-Jerome, C., Bekkelund, S.I., Nordstrom, R., 1997. Quantitative MRI analysis of anatomic dimensions of the carpal tunnel in women. Surgical and Radiologic Anatomy 19 (1), 31–34.

Rempel, D.M., Diao, E., 2004. Entrapment neuropathies: pathophysiology and pathogenesis. Journal of Electromyography and Kinesiology 14, 71–75.

Richman, J.A., Gelberman, R.H., Rydevik, B.L., Gylys-Morin, V.M., Hajek, P.C., Sartoris, D.J., 1987. Carpal tunnel volume determination by magnetic resonance imaging three-dimensional reconstruction. Journal of Hand Surgery 12A, 712–717.

Richman, J.A., Gelberman, R.H., Rydevik, B.L., Hajek, P.C., Braun, R.M., Gylys-Morin, V.M., Berthoty, D., 1989. Carpal tunnel syndrome: morphologic changes after release of the transverse carpal ligament. Journal of Hand Surgery 14A, 852–857.

Rojviroj, S., Sirichativapee, W., Kowsuwon, W., Wongwiwattananon, J., Tamnanthong, N., Jeeravipoolvarn, P., 1990. Pressures in the carpal tunnel. A comparison between patients with carpal tunnel syndrome and normal subjects. Journal of Bone and Joint Surgery 72B, 516–518.

Skie, M., Zeiss, J., Ebraheim, N.A., Jackson, W.T., 1990. Carpal tunnel changes and median nerve compression during wrist flexion and extension seen by magnetic resonance imaging. Journal of Hand Surgery 15A, 934–939.

Smith, E.M., Sonstegard, D.A., Anderson, W.H., 1977. Carpal tunnel syndrome: contribution of flexor tendons. Archives of Physical Medicine and Rehabilitation 58, 379–385.

Weiss, N.D., Gordon, L., Bloom, T., So, Y., Rempel, D.M., 1995. Position of the wrist associated with lowest carpal-tunnel pressure: implications for splint design. Journal of Bone and Joint Surgery 77A, 1695–1699.

Werner, R., Armstrong, T.J., Bir, C., Aylard, M.K., 1997. Intracarpal pressures: the role of finger, hand and forearm position. Clinical Biomechanics 12, 44–51.

Yoshioka, S., Okuda, Y., Tamai, K., Hirasawa, Y., Koda, Y., 1993. Changes in carpal tunnel shape during wrist joint motion. MRI evaluation of normal volunteers. Journal of Hand Surgery 18B, 620–623.

Zeiss, J., Skie, M., Ebraheim, N., Jackson, W.T., 1989. Anatomic relations between the median nerve and flexor tendons in the carpal tunnel: MR evaluation in normal volunteers. American Journal of Roentgenology 153, 533–536.